JOURNAL OF CATALYSIS 112, 313–319 (1988)

NOTES

Electronic Properties of Unsupported Cobalt-Promoted Molybdenum Sulfide

Promotion of sulfided molybdena–alumina HDS catalysts by cobalt and nickel has attracted considerable attention since Richardson demonstrated the existence of "active cobalt," i.e., cobalt not associated with the alumina support or inactive cobalt sulfides (*1*). Although the exact nature of "active cobalt" was not identified, synergistic interaction was shown with a well-defined maximum for activity versus Co_{active}/Mo ratios. A much better understanding of the state of the cobalt has emerged with development of sophisticated characterization techniques such as Mössbauer spectroscopy, XASF, AEM, and others. Topsoe *et al.* recently reviewed current site models and extensive supportive evidence (*2*).

In developing these models, much has been learned from studies on unsupported, promoted MoS_2. Although there are significant differences between the supported and the unsupported catalysts, considerable information may be transferred from investigations on well-characterized bulk materials. Research of this nature was part of the original work reported by Richardson (*1*). Specifically, semiconducting properties of cobalt-promoted, unsupported MoS_2 catalysts were measured in reactive atmospheres and related to thiophene hydrogenolysis kinetics. Results were presented in the patent literature (*3*) but have not received widespread scientific consideration. Only one paper on this subject has appeared, but it was restricted to large crystalline specimens of MoS_2 (*4*). In view of the importance of the earlier work to current models of the active site, it seems appropriate that the results be reexamined in detail.

Six catalysts were prepared with Co/Mo atomic ratios from zero to 0.075. Ammonium paramolybdate was dissolved in 6 *N* NH_4OH and molybdenum sulfide precipitated with H_2S. The suspension was filtered and the precipitate redissolved in distilled water. Three-normal H_2SO_4 was added to precipitate MoS_3, which was then air-dried and divided into six batches and sufficient cobalt acetate solution was added to impregnate the samples with the desired compositions. After wet-mulling for 1 h, the catalysts were air-dried and reduced for 12 h at 873 K in a stream of hydrogen containing 2% H_2S. X-ray diffraction showed very broad lines characteristic of MoS_2 with no evidence of separate phases of cobalt sulfides. Conventional analysis and BET surface area determination gave the results shown in Table 1.

Magnetic susceptibility measurements at 300 K gave -0.59×10^{-6} emu/g for Catalyst No. 1 (Co/Mo = 0), close to the expected value of -0.48×10^{-6} (*5*). Of more interest is promoted Catalyst No. 6, which was the only sample for which measurements were sufficiently accurate to detect cobalt. At 300 K, the magnetic moment, μ_{eff}, was 1.44 μ_B. Chiplunker *et al.* (*6*) reported a value of 1.73 μ_B for sulfided surface cobalt in $CoMo/Al_2O_3$, characteristic of low-spin cobalt in a sulfur environment. However, Topsoe *et al.* (*7*) found 0.75 μ_B for cobalt in the CoMoS state. In view of the difficulty in resolving the cobalt contribution for such low loadings, these discrepancies are not unreasonable. All indicate low-spin, sulfur-complexed cobalt.

Magnetic measurements were used to check catalyst stability during heating in hydrogen. Temperatures above 725 K were

0021-9517/88 $3.00

TABLE 1

Catalyst Characterization

Catalyst	Co/Mo	S_g (m^2/g)
1	0	51
2	0.005	53
3	0.013	56
4	0.029	38
5	0.058	40
6	0.075	35

necessary before any indication of cobalt reduction was detected. Treatments with pure hydrogen in subsequent experiments were all made below 573 K and were considered free from cobalt reduction and phase separation. Thermogravimetric measurements also confirmed that dried samples in both helium and hydrogen did not result in further weight loss upon heating, indicating no decomposition or reduction.

The apparatus and procedure for measuring the electrical conductivity, σ, and the Seebeck coefficient, Q, have been described previously (*8*). Measurements were made from 298 to 673 K under vacuum and in hydrogen and mixtures of various gases.

The experimental procedure was as follows. Each sample was first heated under vacuum at 573 K until temperature, T, conductivity, σ, and QT were constant. These measurements were repeated at decreasing temperatures down to 298 K, after which the sample was returned to 573 K to confirm no change in properties. Hydrogen was admitted to the cell and the equilibrium-measurement cycle was repeated over the same temperature range. The adsorbate was removed at 573 K and vacuum measurements were again taken. Statistical checks showed a precision of from 2 to 5% for all these measurements.

Typical data for Catalyst No. 1 (Co/Mo = 0) are shown in Fig. 1. Other catalyst samples gave similar results.

Measurements of thiophene hydrogenolysis were made in a separate apparatus. Approximately 1 cm^3 (20–40 mesh) of each catalyst was loaded into a 1-cm i.d. quartz tube connected to a conventional flow and chromatographic analytical system. The sample was equilibrated in hydrogen at 573 K and kinetic measurements were started by flowing hydrogen containing 2% thiophene through the tube at increasing flow rates. The usual tests were made to confirm the absence of external and internal diffusion limitations. Conversion decreased initially but reached a steady state after about 30 min. Thereafter, deactivation was negligible, as indicated by frequent checks under starting conditions.

Typical results are shown in Fig. 2. These data were adequately described by a first-order mechanism of the form

$$C_4H_4 \xrightarrow{k_{DS}} C_4^{=} \xrightarrow{k_H} C_4 \qquad (1)$$

from which rate constants for hydrogenolysis and hydrogenation, k_{DS} and k_H, respectively, were determined at 573 K. These measurements were repeated at several temperatures down to 500 K.

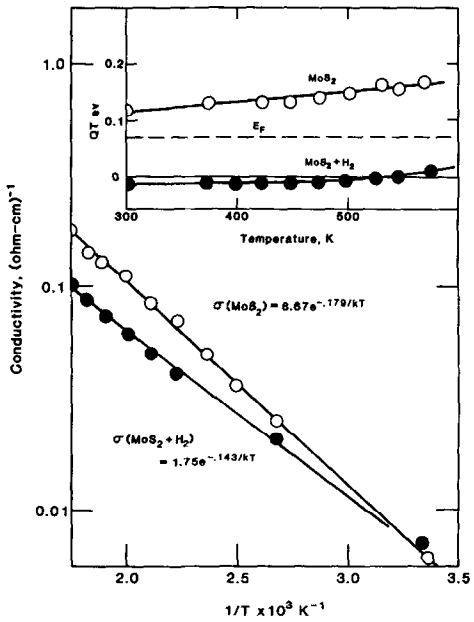

FIG. 1. Conductivity and Seebeck power for Catalyst No. 1 (Co/Mo = 0, under vacuum and in hydrogen).

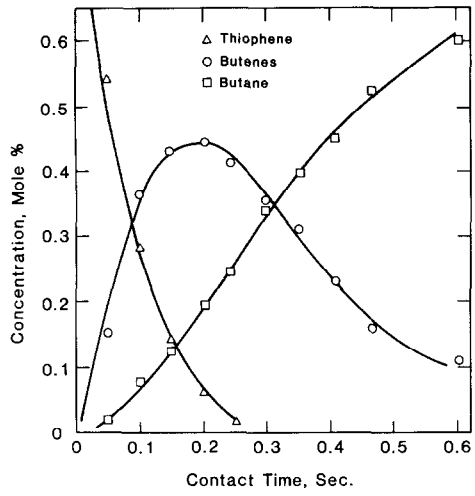

FIG. 2. Kinetic results for Catalyst No. 1 (Co/Mo = 0).

Electrical properties of MoS_2 have been reported, but only for well-crystallized material (*4, 9*). Normally, the crystals are *p*-type semiconductors with an energy gap, E_g, value of 1.45 eV. The morphologies of the catalyst samples listed in Table 1 are not known, but surface areas were moderately high, indicating very small crystallites of approximately 25 nm. Surface effects in large crystals produce bending of energy bands at the surface (*10*). Penetrating to a depth of 10^3 nm, such surface charge regions complicate interpretation of electrical properties. However, Volkenstein has pointed out that when semiconductors decrease in size to dimensions well below this depth, surface effects tend to be diffused and the material responds as a well-behaved, two-dimensional semiconductor (*11*). No frequency dependence of the conductivity was found, indicating that surface charge regions are absent. Interpretation then becomes somewhat easier since less complicated energy band representations may be invoked.

Data in Fig. 3 for the vacuum-treated MoS_2 provide additional information. The value of QT is positive and the temperature dependence of conductivity is accurately described by a single exponential function. These results imply that only one type of charge carrier, positive holes, exists. In these circumstances, QT is given by

$$QT = E_F + 2kT, \tag{2}$$

where E_F is the position of the Fermi level at temperature T and k the Boltzmann constant. Using Eq. (2), the calculated E_F, shown in the insert of Fig. 3, is found to be temperature-independent and located 0.068 eV above the valence band. Acceptor impurities responsible for this *p*-type semiconductivity most likely originate from vacancies in the cationic lattice, each vacant Mo^{4+} ion generating four Mo^{5+} levels.

Upon exposure to 1 atm of hydrogen at 573 K, QT decreased very quickly, achieving steady state within 30 s and became negative at low temperatures. This indicates a change in semiconductivity produced by the appearance of negative charge carriers. For two types of carriers, QT becomes (*10*)

$$QT = E_F\sigma_p - (E_g - E_F)\sigma_n + 2kT(\sigma_p - \sigma_n) \tag{3}$$

with

$$\sigma = \sigma_p + \sigma_n, \tag{4}$$

where σ_n is the electron and σ_p the positive

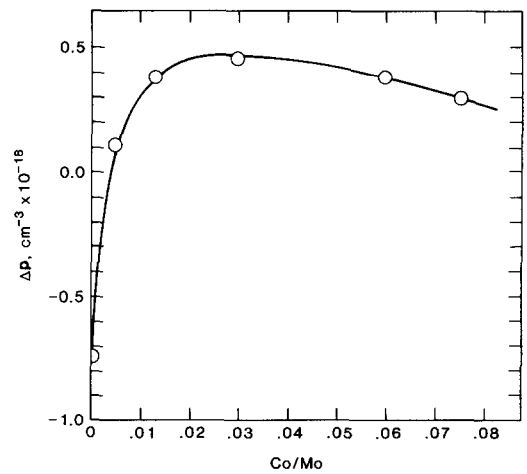

FIG. 3. Effect of hydrogen adsorption on *p*.

hole conductivity. The positive charge conductivity is given by (*10*)

$$\sigma_p = e\mu_p N_V \exp(-E_F/kT), \quad (5)$$

where e is the electronic charge, μ_p the positive charge mobility, and N_V the density of states. These last two constants may be determined at each temperature from the conductivity under vacuum. Equations (3), (4), and (5) were combined to determine the parameters E_F, σ_p, and σ_n from the measurements of QT and σ.

The positive and negative charge conductivities are related to the charge densities by

$$\sigma_p = e\mu_p p \quad (6)$$

and

$$\sigma_n = e\mu_n n \quad (7)$$

where p and n are the charge densities of positive and negative carriers, respectively, and μ_p and μ_n are the charge mobilities. Values for μ_p are known from the analysis so that p may be found. However, to deduce n, it is necessary to assume $\mu_p \approx \mu_e$. If this is not correct, then adjustments in the values of n are required, but the trends are the same.

From these simple measured quantities, it is possible to deduce estimates of p and n for each sample, with and without hydrogen treatment. Patterns may then be used to diagnose the effects of promotion. For example, Table 2 shows the effect of hydrogen adsorption on unpromoted MoS_2.

Table 2 shows that hydrogen adsorption decreases p but increases n and that the effect is irreversible. This indicates a reaction of the type

$$H_2 + S^{2-} = (H_2S)_{ads} + 2e \quad (8)$$

which removes S^{2-} ions from the lattice. The electrons neutralize acceptor levels and create donor levels to account for the observed conductivity changes.

Since exposure to hydrogen at reaction temperatures leads to generation of sulfur vacancies, activation is a consequence of H_2S/H_2 ratios through equilibrium Reaction (8) and

$$(H_2S)_{ads} = H_2S \quad (9)$$

The implications of these experiments are crucial in understanding the activated state of MoS_2. Initial or "fresh" activity is determined by the H_2S/H_2 ratio and temperature during sulfiding. Thereafter, the catalyst responds to changes in the sulfur–hydrogen environment. For example, the initial activity decreases during the early phases of thiophene hydrogenolysis. Although deactivation could be due to coke formation, it is possible that equilibrium between hydrogen and sulfur via sulfur vacancies is taking its toll of active sites. It is even possible that activation could occur under the right conditions. Thus, activity is a consequence of gas composition, temperature, and, indirectly, extent of conversion.

Promotion of MoS_2 by altervalent cobalt is equivalent to electronic "doping" of the semiconductor by (i) intercalation, (ii) cationic vacancy substitution, or (iii) molybdenum substitution. Examination of changes in p and n during cobalt substitution allows discrimination between these possibilities. Obviously, all three could coexist and confound the interpretation, yet the principal mechanism is indicated from data given in Table 3.

Intercalation of cobalt into interstitial positions is expected to generate donor levels and increase negative charge concentration. This occurs to some extent, but the change is relatively small and appears to be constant after the initial increase. The most

TABLE 2

Effect of Hydrogen Adsorption on MoS_2

Atm	QT (eV)	σ (ohm-cm)	E_F (eV)	$p \times 10^{-18}$ (cm^{-3})	$n \times 10^{-18}$ (cm^{-3})
Vac	0.166	0.182	0.068	1.36	0
H_2	−0.003	0.0944	0.117	0.612	0.049
Vac	0.034	0.102	0.102	0.687	0.075

Note. Temperature = 573 K.

TABLE 3

Cobalt Promotion of MoS_2

Co/Mo	E_F (eV)	$p \times 10^{-18}$ (cm^{-3})	$n \times 10^{-18}$ (cm^{-3})
0	0.068	1.36	0
0.005	0.127	0.493	0.026
0.013	0.174	0.220	0.032
0.029	0.193	0.126	0.015
0.058	0.209	0.076	0.013
0.075	0.225	0.048	0.024

Note. Vacuum, 573 K.

significant change is the decrease in positive charge concentration. Substitution of lattice molybdenum by cobalt creates acceptor levels and would increase the positive charge concentration. Cobalt insertion into molydenum vacancies, however, should decrease the number of acceptor levels and decrease positive charge concentration. Although all three substitution modes appear to occur, the dominant result is vacancy substitution. It is not possible from these data alone to determine whether basal or edge cationic sites are involved.

Hydrogen adsorption at 573 K gave the parameters shown in Table 4. Several significant observations should be emphasized. First, the decrease in p noted for the nonpromoted sample is not so pronounced. Second, there is a substantial increase in negative charge n with addition of cobalt promoter.

Hydrogen interaction is very different in the presence of cobalt. Figure 3 shows the hydrogen-induced change in p as a function of cobalt concentration. Without cobalt, hydrogen removes lattice sulfur through Reaction (8) and a decrease in p results. However, hydrogen interacts with cobalt (predominantly in lattice positions) to increase the number of acceptor levels. This implies a localization of the hydrogen of the type

$$H_2 + Co^{2+} = (2H\text{–}Co)^0 \qquad (10)$$

The effect is most pronounced in the early phase of cobalt addition, reaching a maximum value at Co/Mo = 0.03. Above this point, the observed trend may be due to diffusion of cobalt into the interior lattice positions, inaccessible to hydrogen.

Table 4 also shows an increase in n from formation of sulfur vacancies via Reactions (8) and (9) but facilitated by cobalt. Thus promotional effects include generation of hydrogen ions, acceptor sites, and sulfur vacancies through mechanisms not found for unpromoted catalysts. In all cases, the electronic changes were essentially irreversible, so that the hydrogen ions are very strongly held and do not desorb under these conditions.

Rate constants for hydrogenolysis and hydrogenation are shown in Fig. 4 for measurements at 573 K. The most dramatic effect is the increase in hydrogenolysis with Co/Mo ratio by a factor of 10^2. Hydrogenation, however, shows only a very slight increase. These results are very similar to those reported by Topsoe *et al.* (*2*). Hydrogenolysis is promoted by cobalt whereas hydrogenation is not.

Compensation effects were found in the hydrogenolysis kinetic constants, as shown in Table 5. These effects have been observed by others yet the significance is not clear (*12*).

This research suggests that molybdenum sulfide crystallites approaching the size found in supported catalysts behave very much like two-dimensional semiconduc-

TABLE 4

Cobalt Promotion of MoS_2

Co/Mo	E_F (eV)	$p \times 10^{-18}$ (cm^{-3})	$n \times 10^{-18}$ (cm^{-3})
0	0.117	0.612	0.049
0.005	0.138	0.600	0.100
0.013	0.138	0.600	0.100
0.029	0.140	0.576	0.102
0.058	0.152	0.452	0.102
0.075	0.165	0.347	0.104

Note. 573 K, 1 atm H_2.

tors. For the fresh, unpromoted material, conduction is caused by acceptor levels produced by molybdenum ion vacancies. Sulfur vacancies are not present in sufficient quantity to impart *n*-type conductivity via donor levels. Exposure to hydrogen generates sulfur vacancies, believed to be catalytic sites, at a concentration consistent with thermodynamic equilibrium among a number of reactions. Thus the activity of the catalyst is conditioned by the composition and temperature of the reacting environment.

Addition of cobalt profoundly increases hydrogenolysis activity but leaves butene hydrogenation relatively unchanged. Thus cobalt promotion must be restricted to the thiophene adsorption and conversion step, with subsequent hydrogenation, perhaps on a separate site, determined by the characteristics of the host lattice. The degree of enhancement suggests that cobalt promoters are readily accessible to reacting thiophene (i.e., at the surface) and are located at edge positions in the lattice. This is confirmed by electronic parameters which indicate that cobalt occupies vacant molybdenum lattice positions most likely situated at the edge of the basal planes. Cobalt does not intercalate to any large degree that can be correlated with activity.

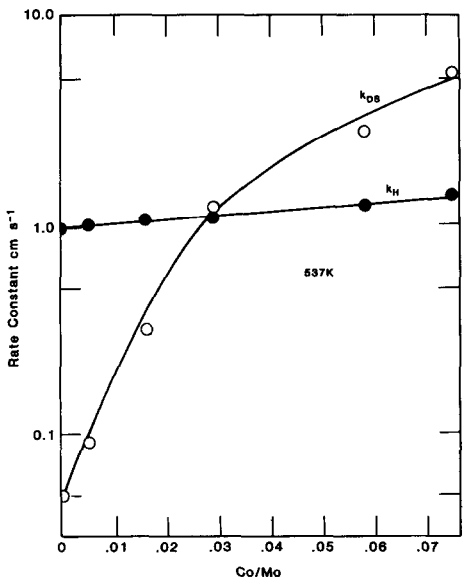

FIG. 4. Thiophene hydrogenolysis and hydrogenation.

TABLE 5

Compensation Effect for Hydrogenolysis Rate Constant Parameters

Co/Mo	$k_{DS,o}$ (cm s^{-1})	E_{DS} (kJ/mole)
0	1.00×10^7	87.9
0.005	1.58×10^7	83.7
0.013	7.94×10^9	109
0.029	3.98×10^{12}	130
0.058	1.58×10^{13}	134
0.075	2.51×10^{14}	142

The promotional effect of cobalt is best seen in its interaction with hydrogen, which is entirely different from the unpromoted MoS_2. Hydrogen is dissociated to a very strongly bound form which generates sulfur vacancies and creates more acceptor levels. These defects do not, however, correlate directly with hydrogenolysis activity so that other factors must prevail. One very definite possibility is that the rate of hydrogen dissociation may be sufficiently enhanced so that sulfur removal, or regeneration of the active site, proceeds at a much faster rate. The nature of the hydrogenation site still needs to be deciphered.

ACKNOWLEDGMENTS

This research was carried out in the laboratories of the Research Department Humble Oil and Refining Co., later Exxon Research and Engineering. Special thanks are due to Dr. L. W. Vernon who performed the thiophene kinetic experiments.

REFERENCES

1. Richardson, J. T., *Ind. Eng. Chem. Fundam,* **3,** 154 (1964).
2. Topsoe, H., Candia, R., Topsoe, N-Y., and Clausen, B. S., *Bull. Soc. Chim. Belg.* **93,** 783 (1984).
3. Vernon, L. W., and Richardson, J. T., U.S. Patent 3,000,816 (June 24, 1959).
4. Wentrcek, P. R., and Wise, H., *J. Catal.* **51,** 80 (1978).

5. Belougne, P., Zanchetta, J. V., and Rouillon, J. D., *J. Chim. Phys. Physiocochim. Biol.* **70,** 683 (1973).
6. Chiplunker, P., Martinez, N. P., and Mitchell, P. C. H., *Bull. Soc. Chim. Belg.* **90,** 1319 (1981).
7. Topsoe, H., Topsoe, N.-Y., Sorensen, O., Candia, B., Calusen, B. S., Kallesoe, S., Pedersen, E., and Nevald, R., *Amer. Chem. Soc. Div. Pet. Chem. Repr.* **28,** 5 (1983).
8. Richardson, J. T., *J. Catal.* **6,** 328 (1966).
9. Mansfield, R., and Salam, S. A., *Proc. Phys. Soc. B.* **66,** 377 (1953).
10. Hannay, N. B., "Semiconductors." Reinhold, New York, 1959.
11. Volkenstein, F. F., "The Electronic Theory of Catalysis on Semiconductors." MacMillan Co., New York, 1963.
12. Mithcell, P. C. H., and Scott, C. E., *Bull. Soc. Chim. Belg.* **93,** 619 (1984).

JAMES T. RICHARDSON

Department of Chemical Engineering
University of Houston
Houston, Texas 77004

Received June 10, 1987; revised February 2, 1988